YBCO grain boundary Josephson junction coupled with a slot dipole antenna for terahertz wave detectors

H Yamada, T Hayasaka, G Toya, A Saito, S Ohshima and K Nakajima

Yamagata University, 4-3-16 Jonan, Yonezawa-shi, Yamagata 992-8510, Japan

E-mail: hyamada@yz.yamagata-u.ac.jp

Abstract. We examined terahertz wave detectors that used $YBa_2Cu_3O_{7-\delta}$ (YBCO) grain boundary Josephson junctions (GBJJs) coupled with a slot dipole antenna (SDA). The detectors consisted of a 220-GHz full-wavelength SDA patterned on a Au layer and a GBJJ patterned on an YBCO/bicrystal MgO film, which were separated by an insulating benzocyclobutene layer. The microbridge of the fabricated junction was 5-μm wide and was trimmed to 2 μm using an ultraviolet laser cutter to modify the junction parameters. The critical current I_C, normal resistance R_N, and I_CR_N product after the trimming at 30 K were 0.62 mA, 1.42 Ω, and 0.88 mV, respectively. The current–voltage characteristics and radio frequency (RF) wave responses of these detectors for a millimeter wave of 180–240 GHz were measured at 30 K. The coupling efficiency between the GBJJ and the SDA and the system sensitivity were obtained as -19.0 dB and 630 V/W, respectively, at 193 GHz. For the RF wave response of 180–240 GHz, the coupling efficiency was relatively flat.

1. Introduction

Terahertz wave, which is an electromagnetic wave of approximately from 100 GHz to 10 THz, has the transparency of radio wave and straightness of optical wave. It features absorption lines that vary with the materials. Therefore, the terahertz wave can be used in some applications such as in imaging [1] and biological and chemical analyses [2]. Terahertz wave can be detected using semiconductor detectors, e.g., Si bolometer and Schottky barrier diode detector, or low-temperature superconductor (LTS) detectors, e.g., superconductor bolometer [3] and kinetic inductance detector [4]. These detectors have their own advantages and disadvantages. For example, the Si bolometer has a wide detection-frequency range, but its working temperature is only a few Kelvin because of thermal noise. The Schottky barrier diode detector can operate at room temperature, but its detection-frequency range is limited. Finally, the LTS detectors have higher sensitivity than the semiconductor detectors; however, their working temperature is only a few Kelvin owing to superconducting transition. Therefore, more sensitive general-purpose detectors are desired.

We have been examining high-temperature superconductor Josephson junction detectors because they can operate at liquid nitrogen temperature (77 K) and have high sensitivity around the terahertz wave band. We have reported on detectors coupled with two sets of half-wavelength (λ/2) slot dipole antenna (SDA) and a coplanar waveguide (CPW) [5]. The λ/2 SDAs have relatively low feed-point impedance, but as a detector, the CPWs have a limited bandwidth. Therefore, to develop wide band and sensitive terahertz detectors, we propose the grain boundary Josephson junction (GBJJ) detectors with a full-wave length (1λ) SDA without a CPW [6]. In this paper, we report the results of our

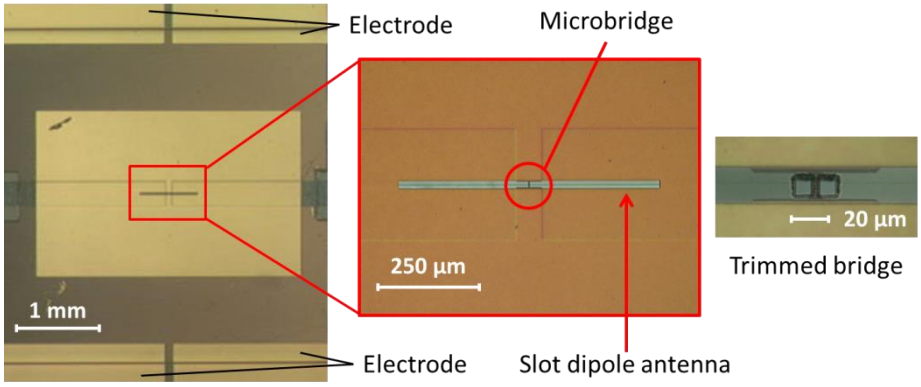

Figure 1. Optical microscope images of the fabricated single 1λ-SDA-coupled GBJJ detector.

Table 1. Characteristics of the junction to the bridge width.

Bridge width w (μm)	Critical current I_C (mA)	Normal resistance R_N (Ω)	$I_C R_N$ (mV)
5	1.30	0.62	0.81
3	0.68	1.06	0.72
2	0.62	1.42	0.88

examination on the coupling efficiency between a 1λ SDA designed for 220 GHz and the GBJJ, as well as the system sensitivity of the detector.

2. Experimental

The 1λ-SDA-coupled GBJJ detectors were made of Au (50 nm)/$YBa_2Cu_3O_{7-\delta}$ (YBCO, 100 nm)/bicrystal MgO (0.5 mm) films using Ar ion etching with photolithography. Initially, a 5-μm-wide YBCO microbridge was fabricated across the grain boundary of the MgO substrate. Next, the Au layer was etched to remove the Au on the junction and to fabricate four electrodes. Then, an insulating benzocyclobutene (BCB) layer was fabricated on the bridge and the bared MgO. Finally, a Au layer was deposited on the BCB layer by sputtering, and a 1λ SDA designed at 220 GHz, whose feed-point impedance Z_{ANT} was simulated as $3 + j20$ Ω, was fabricated.

The microbridges of the fabricated detectors were trimmed using ultraviolet laser etching to improve the junction characteristics. Thereafter, the current–voltage (I–V) characteristics of the detectors were evaluated. The detectors were cooled down to approximately 30 K using a pulse tube cryocooler, and an alternating current was applied to the junction to measure the voltage using an oscillator. In addition, the response was measured for the radio frequency (RF) wave of 180–240 GHz. The RF wave was generated using a Gunn diode signal generator (30–40 GHz) that reached the detector via an amplifier (30 dB), frequency multipliers (a total of six times), horn antenna, polymethilpentene lens, parabolic mirror, and hyperhemispherical Si lens.

3. Results and discussions

Figure 1 shows the optical microscope images of the fabricated single 1λ-SDA-coupled GBJJ detector. The length and width of the antenna slot and the thickness of the BCB layer were 700, 20, and 2.5 μm, respectively. Table 1 lists the characteristics of the junction for the 5-, 3-, and 2-μm-wide microbridges, which were obtained from the I–V characteristics. As the width of the bridge became thinner, the critical current I_C decreased, and the normal resistance R_N increased. However, the value of the product of I_C and R_N was almost constant, which was approximately 0.8 mV.

Figure 2 shows the RF wave responses measured at 30 K and 193 GHz for the 5- and 2-μm-wide bridges. Although the RF power values P_{RF} irradiated to the antenna were almost the same, the

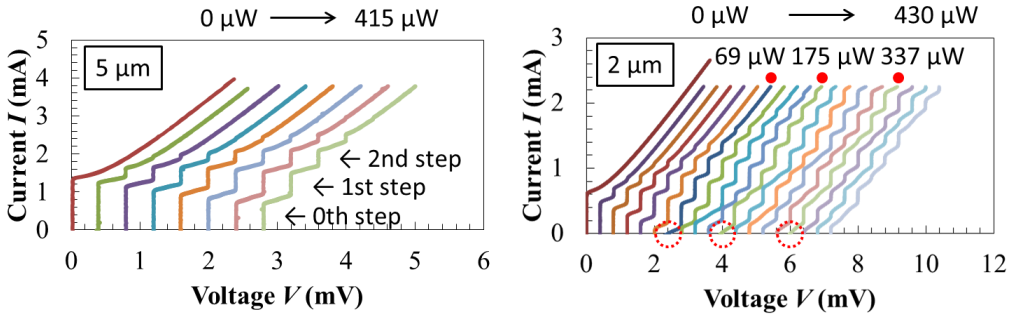

Figure 2. RF wave responses of the detectors for the 5- and 2-μm-wide bridges at 30 K and 193 GHz. Each characteristic is shifted to the right-hand side by 0.4 mV as the power decreased.

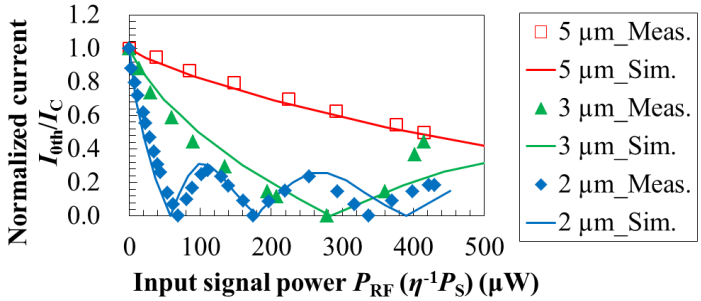

Figure 3. Characteristics of the current at the zeroth step I_{0th} to irradiated RF power P_{RF}. The I_{0th} values are normalized by each critical current I_C measured at P_{RF} = 0.

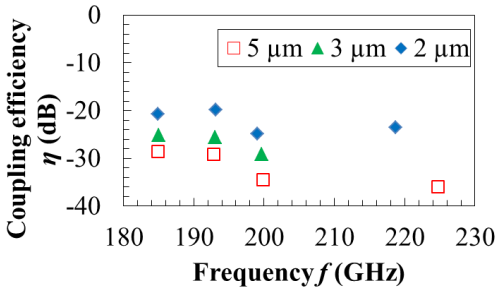

Figure 4. Frequency characteristics of coupling efficiency η for the bridge width at 30 K.

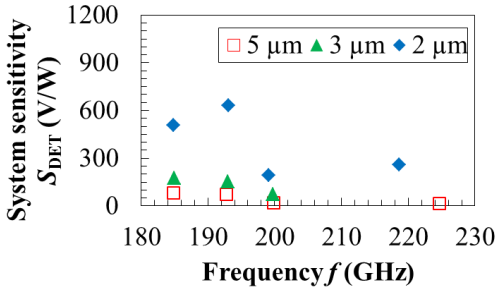

Figure 5. Frequency characteristics of system sensitivity S_{DET} for the bridge width at 30 K.

variations in the Shapiro steps to the power were different. Figure 3 shows the characteristics of the current in the zeroth step I_{0th} to the P_{RF}. For the 5-μm width, the I_{0th} values decreased monotonically with the RF power and did not reach 0 mA. Meanwhile, for the 2-μm width, the I_{0th} values alternately decreased and increased and became 0 mA three times, which means that the coupling between the junction and the antenna was improved by the trimming of the bridge.

To quantitatively evaluate the coupling between the junction and the antenna, the RF response of the Josephson junction was simulated using a resistively shunted junction model, which yielded the following equation:

$$I + I_S \sin 2\pi f_S t = I_C \sin\theta + \frac{V}{R_N}, \quad (1)$$

where I, I_S, f_S, t, θ, and V are the current, input signal current, input signal frequency, time, phase difference, and voltage, respectively. From the simulation, the I–V characteristics and the power introduced to the junction P_S (= $R_N I_S^2/2$) were obtained. The coupling efficiency η was obtained by fitting P_{RF} to P_S and was defined as P_S/P_{RF}. The I_{0th} value of P_S, which was fitted by multiplying η^{-1}, is also shown in Figure 3. Because the variations in the measured I_{0th} values agreed well with those of the fitted I_{0th} values, we believe that the effect of noise on the measured values was low. Figure 4 shows the frequency dependence of the coupling efficiency. The coupling efficiency increased as the bridge became thinner and was approximately -19 dB at 193 GHz for the 2-μm-wide bridge. We believe that this effect was caused by the improvement in the impedance matching because the normal resistance of the junction was enlarged by approximately 2.3 times and approached the impedance of the antenna. The values of the impedance mismatching loss M, which were estimated from the following equation:

$$M = 10\log_{10}\left(1-|\Gamma|^2\right), \quad \Gamma = \frac{Z_{ANT}-R_N}{Z_{ANT}+R_N}, \tag{2}$$

were -17.4 and -13.9 dB for the 5- and 2-μm-wide bridges, respectively. Although the impedance mismatching loss improved by approximately 3.5 dB, each loss value could be high. We believe that the Z_{ANT} reactance enlarged the impedance; thus, we need to examine the structure of the antenna or the whole detector. The frequency characteristics of the coupling efficiency slightly decreased with the frequency, but they were relatively flat. We believe that this is beneficial for wide-band detector.

Figure 5 shows the system sensitivity S_{DET} calculated by the following equations:

$$S_{DET} = \eta S, \quad S = \frac{\Phi_0}{16\pi k_B T}\frac{2f_C^{\,2}}{2f_S^{\,2}+3f_C^{\,2}}, \quad f_C = \frac{I_C R_N}{\Phi_0}. \tag{3}$$

In these equations, S, Φ_0, k_B, T, and f_C are the sensitivity, flux quantum, Boltzmann constant, device temperature, and junction characteristic frequency, respectively. The highest S_{DET} value was obtained as approximately 630 V/W at 193 GHz for the 2-μm-wide bridge. This value is yet lower than that of the Schottky barrier diode detectors. We are going to improve the system sensitivity by examining in details the effects of thinning the bridge width on the improvement of the coupling efficiency.

4. Summary

A single 1λ-SDA-coupled YBCO GBJJ detector (220 GHz, 5-μm-wide microbridge) has been fabricated. The bridge was thinned by laser etching, and the highest coupling efficiency of approximately -19 dB was obtained for the 2-μm-wide bridge at 30 K and 193 GHz. Here, the highest system sensitivity was approximately 630 V/W. The coupling efficiency increased as the bridge became thinner. For an RF wave response of 180–240 GHz, the coupling efficiency was relatively flat.

Acknowledgments

This work was supported by JSPS KAKENHI Grant Number 24760313. A part of this work was carried out in the clean room of Yamagata University.

References

[1] Du J, Hellicar A D, Li L, Hanham S M, Macfarlane J C, Leslie K E, Nikolic N, Foley C P and Greene K J 2009 *Supercond. Sci. Technol.* **22** 114001
[2] Kawase K, Ogawa Y, Watanabe Y and Inoue H 2003 *Opt. Express* **11** 2549-2554
[3] Liu L, Xu H, Percy R R, Herald L L, Lichtenberger A W, Hesler J L and Weikle R M II 2009 *IEEE Trans. Appl. Supercond.* **19** 282-286
[4] Day P K, LeDuc H G, Mazin B A, Vayonakis A and Zmuidzinas J 2003 *Nature* **425** 817-821
[5] Nakajima K, Ebisawa N, Sato H, Chen J, Yamashita T and Sawaya Y 2005 *IEEE Trans. Appl. Supercond.* **15** 549-551
[6] Yamada H, Hayasaka T, Saito A, Ohshima S and Nakajima K 2013 *Physics Procedia* **45** 217-220